

Supporting Information for

Ruthenium photosensitizer anchored gold nanorod for synergistic photodynamic and photothermal therapy

Hongdong Shi,[‡] Simin Lin,[‡] Yi Wang, Jingxue Lou, Yatao Hu, Yuyu Chen and Qianling Zhang*

Graphene Composite Research Center, College of Chemistry and Environmental Engineering, Shenzhen University, Shenzhen, Guangdong 518060, China.

email: zhql@szu.edu.cn

Content

Scheme S1. Synthetic routes to $[\text{Ru}(\text{bpy})_2(\text{AIPF-formaldehyde})]\text{Cl}_2$.

Fig. S1 $^1\text{H-NMR}$ spectrum of NPIP.

Fig. S2 $^1\text{H-NMR}$ spectrum of APIP.

Fig. S3 $^1\text{H-NMR}$ spectrum of $[\text{Ru}(\text{bpy})_2(\text{AIPF})]\text{Cl}_2$.

Fig. S4 Identification of $[\text{Ru}(\text{bpy})_2(\text{AIPF})]^{2+}$ by ESI/QTOF

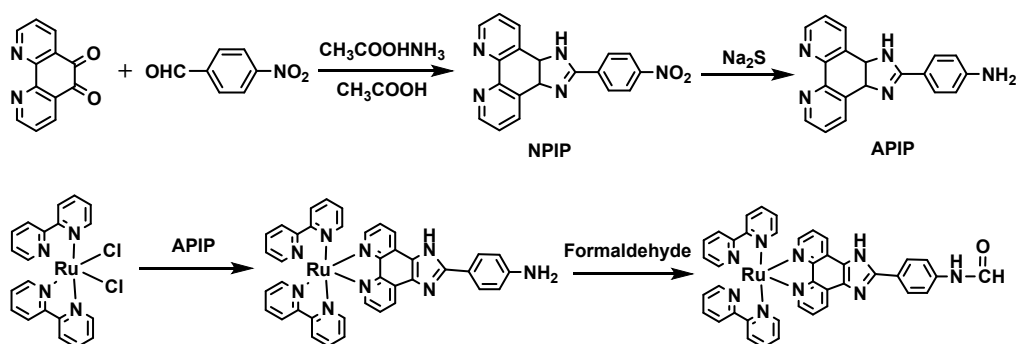
Table S1. Growth conditions for gold nanorods.

Fig. S5 The normalized absorption spectra of GNRs and GNR-HSANPs in aqueous solutions.

Fig. S6 Ru release study of Ru-GNR-HSANPs.

Fig. S7 Cellular uptake of Ru and Ru-GNR-HSANP measured by fluorescence microscopy

Fig. S8 Photodynamic therapy effect of Ru and Ru-GNR-HSANPs.



Scheme S1. Synthetic routes to $[\text{Ru}(\text{bpy})_2(\text{AIPF-formaldehyde})]\text{Cl}_2$.

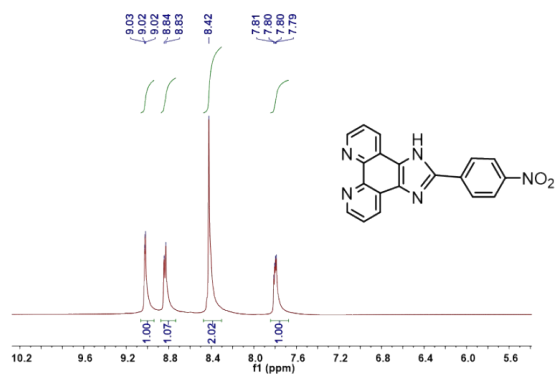


Fig. S1 $^1\text{H-NMR}$ spectrum of 2-(4-nitrophenyl)-1H-imidazo[4,5-f][1,10]-phenanthroline (NPIP) in $\text{d}^6\text{-DMSO}$. All of 5 unique signals from aromatic groups were observed, two of which were overlapped.

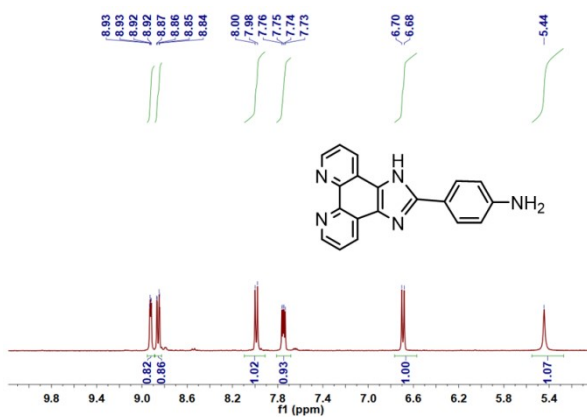


Fig. S2 $^1\text{H-NMR}$ spectrum of 2-(4-aminophenyl)-1H-imidazo[4,5-f][1,10]-phenanthroline (APIP) in $\text{d}^6\text{-DMSO}$. All of 5 unique signals from aromatic groups were observed. The 5.44 ppm peak is the NH_2 signal.

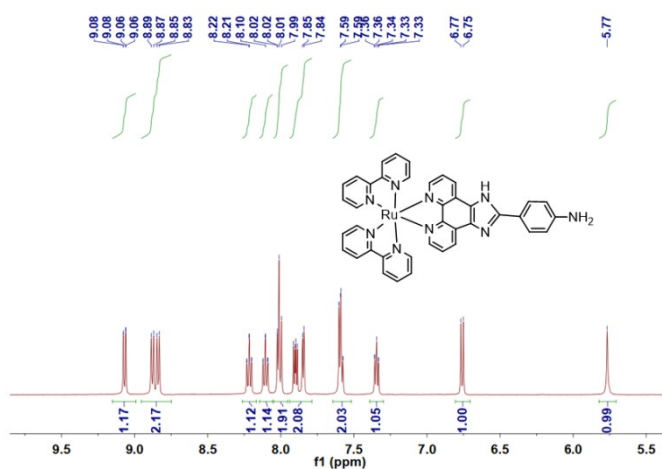


Fig. S3 $^1\text{H-NMR}$ spectrum of $[\text{Ru}(\text{bpy})_2(\text{APIP})]\text{Cl}_2$ in $\text{d}^6\text{-DMSO}$. All of 9 unique signals from aromatic groups were observed. The 5.77 ppm peak is the NH_2 signal.

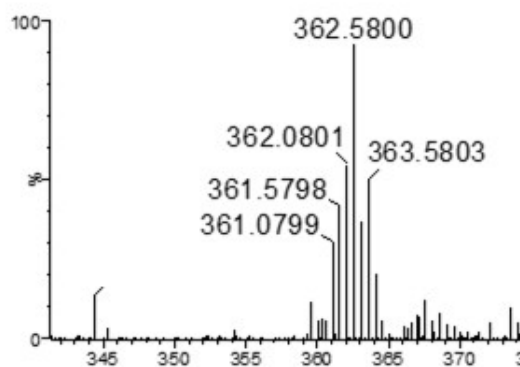


Fig. S4 Identification of $[\text{Ru}(\text{bpy})_2(\text{APIP})]^{2+}$ by ESI/QTOF, m/z : Calcd for $\text{C}_{39}\text{H}_{29}\text{N}_9\text{Ru} [\text{M}]^{2+}$ 362.5794; found 362.58.

Table S1. Growth conditions for gold nanorods with different LSPR wavelengths.

LSPR wavelength (nm)	CTAB (g)	AgNO ₃ (mL)	Seed (mL)	HCl (mL)	NaOL (g)
780	9	12	0.4	1.5	1.543
800	9	12	0.4	2.1	1.543
808	7	18	0.4	1.5	1.234
900	7	12	0.4	1.5	1.234

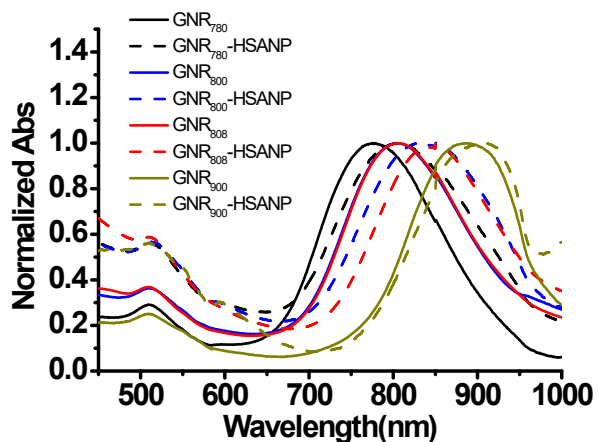


Fig. S5 The normalized absorption spectra of GNRs (solid lines) and GNR-HSANPs (dashed lines) in aqueous solutions. The redshift phenomenon was observed by HSA coated GNRs, compared with GNRs.

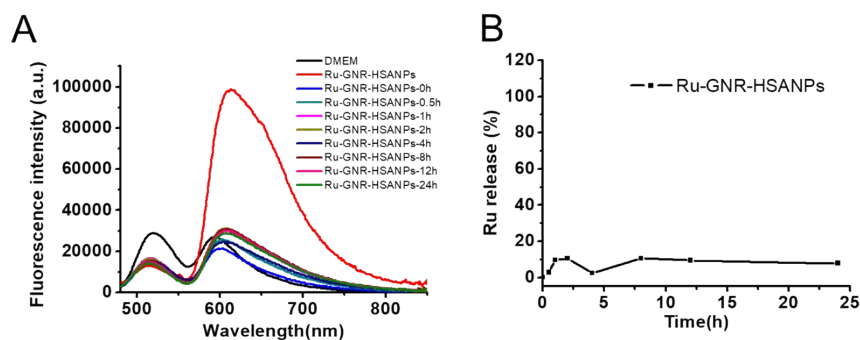


Fig. S6 Ru release study of Ru-GNR-HSANPs. 50 μ L of Ru-GNR-HSANPs solution was mixed with 200 μ L DMEM/FBS solution. After incubation for different times (0, 1, 2, 4, 8, 12, 24 h), the supernatant was collected by centrifugation. (A) The fluorescence of supernatant was measured. (B) the Ru release kinetic from Ru-GNR-HSANPs was calculated.

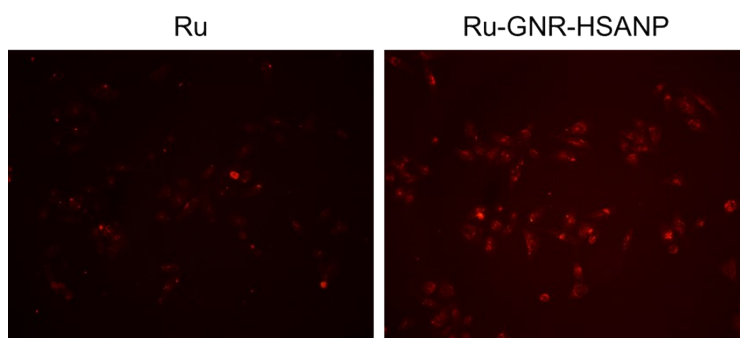


Fig. S7 Cellular uptake of Ru and Ru-GNR-HSANP. HepG2 cells were treated with Ru and Ru-GNR-HSANP (Ru concentration: 50 μ M). After incubation for 4 h, the drugs were removed and washed with PBS for three times. The cellular uptake of Ru and Ru-GNR-HSANP was measured by fluorescence microscopy.

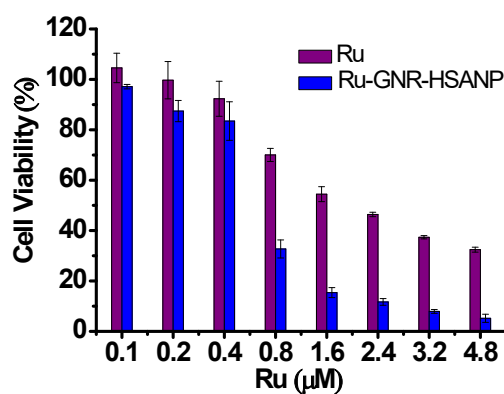


Fig. S8 Photodynamic therapy effect of Ru and Ru-GNR-HSANPs. HepG2 cells were incubated with Ru or Ru-GNR-HSANPs with different Ru concentrations for 4 h and then irradiated with 465 nm light (6.5 mW/cm², 25min). After culturing for 24, cell viability was measured by MTT assay.